Optical OFDMA for Multi-cell/Multi-User Indoor Optical Wireless Networks

Michael Rahaim*, Arsalan Ahmed**, Michel Kulhandjian†, and Hovannes Kulhandjian‡
*Engineering Department, University of Massachusetts, Boston, MA U.S.A.
**Deutsche Telekom, Friedrich-Ebert-Allee 140 53113, Bonn, Germany
†Department of Electrical and Computer Engineering, Rice University, Houston, TX U.S.A.
‡Department of Electrical & Computer Engineering, California State University, Fresno, Fresno, CA 93740, U.S.A.
E-mail: michael.rahaim@umb.edu

***Abstract*—The research community continues to explore indoor optical wireless communications (OWC) as a potential candidate for increased network capacity in future networks. Much progress has been made in the area of high-speed point-to-point OWC links; however, there are still significant open challenges related to the allocation of resources in dynamic multi-cell and multi-user environments. In this work, we develop and demonstrate a multi-user DC-biased Optical OFDMA (DCO-OFDMA) implementation to dynamically allocate subcarriers across multiple OWC links.**

Our DCO-OFDMA codebase is integrated in the gr-owc library as an extension of the broadly used GNURadio software toolkit, along with a set of example flowgraphs for applying DCO-OFDMA in practice. Our implementation has been evaluated for various environments in simulation using the gr-owc optical wireless channel module, and experimentally using USRP hardware for SDRs with custom front-end OWC transmitter/receiver hardware. As a result, we provide an experimental analysis framework for DCO-OFDMA concepts that exist in the literature. More relevantly, we offer a testbed model with an easy-to-use and relatively low-cost design that allows for similar multi-cell/multi-user systems to be experimentally evaluated.

***Index Terms*—Optical Wireless Communication (OWC), Software Defined Radio (SDR), Multiple Access, Orthogonal Frequency Division Multiplexing (OFDM)**

I. Introduction

The wireless communications ecosystem is continuously evolving, with novel devices and applications driving the demand for additional wireless capacity. The research community is interested in optical wireless communications (OWC) as a candidate technology to address this growing demand and high-speed point-to-point OWC links have been demonstrated. Researchers have also developed novel modulation schemes for OWC by adapting conventional orthogonal frequency division multiplexing (OFDM) techniques to meet the constraints of the optical channel [1]. Beyond the high rate capability of OWC links, the optical channel's directionality also enables an ultra-dense distribution of OWC access points (APs). This allows for unprecedented area capacity (b/s/m^2) in multi-cell and multi-user environments.

While directionality provides some isolation of OWC links, network deployment should still account for tradeoffs between coverage overlap and interference effects. Accordingly, resource allocation techniques are required to define how OWC resources are shared across cells and across users within a given cell. The use of OFDM subcarrier allocation for multiple access (i.e., OFDMA) has been broadly explored for RF communications and is a key aspect of 5G, but there is significantly less work in the application of OFDMA for OWC.

In this paper, we first provide a detailed comparison of the RF and OWC signal chains for OFDM / OFDMA. We also introduce two novel contributions. First, we describe the addition of an optical OFDMA module and test code / test setup within our openly available software library for OWC. The library (namely, *gr-owc*) is developed within the widely used GNURadio software toolkit for software-defined radio (SDR) and allows for software simulation and experimental testing of OWC systems using SDR hardware [2], [3], [4]. Second, we apply DCO-OFDMA in a simulated OWC network to evaluate the packet-layer performance in comparison with full resource reuse scenarios under different operating conditions. These simulated scenarios are validated in a small-scale experimental setup using commercially available SDR hardware (universal software radio peripheral or USRP) with additional front-end OWC hardware for visible light communications (VLC).

II. Background

Before introducing our contributions, we first review the unique characteristics of RF OFDMA and the optical OFDM techniques that are applied in our work. We also provide an introduction to other resource allocation methods considered by the OWC community, and introduce our prior work in applying SDR techniques to OWC in order to develop openly available real-time signal processing tools for OWC research.

A. OFDM and OFDMA

OFDM applies frequency division multiplexing to orthogonal subcarriers [5], allowing for highly efficient multi-carrier data transmission. The high-level process for generating a conventional OFDM frame, Fig. 1, is as follows. First, the desired bit sequence is divided across multiple active subcarriers, and the bits assigned to each subcarrier are mapped to a corresponding (potentially) complex-valued *subcarrier symbol*. The symbols are passed through an inverse FFT module. This includes any pilot symbols on the desired pilot carriers and zeros on any inactive subcarriers, in order to generate a complex-valued time domain signal. The total number of

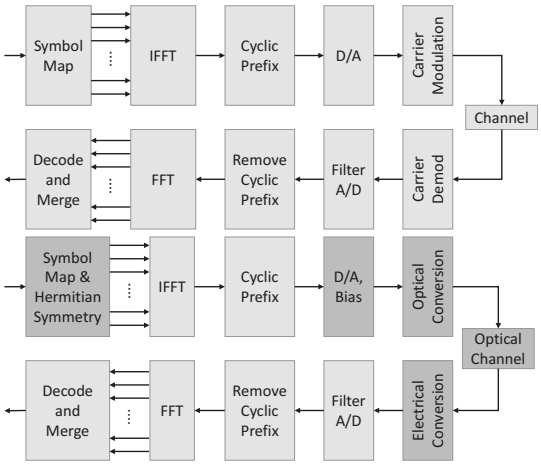

Fig. 1. Single link signal chain for a conventional OFDM Tx/Rx implementation (*top*) and a DC-biased Optical OFDM Tx/Rx implementation (*bottom*).

subcarrier symbols (i.e., active, inactive, and pilot subcarriers) per *OFDM symbol* should be equal to the FFT size, N_{FFT}. A cyclic prefix is then added as a guard interval to mitigate intersymbol interference (ISI). Finally, the complex baseband signal is carrier-modulated to center the signal at a desired frequency. At the receiver, the process is reversed. However, the receiver must also account for timing and synchronization issues introduced by the channel and hardware. In practice, packetization is implemented on top of this such that multiple OFDM symbols combine to form an *OFDM Frame*. The bit sequence associated with a single frame includes the relevant information to be transmitted, along with a frame header that incorporates control information and error coding.

Since symbols are individually assigned to different subcarriers, the OFDM waveform structure is well suited for multiple access implementations where separate symbol sequences are assigned to different subcarrier sets (i.e., OFDMA). Synchronization of the transmitted subcarrier waveforms is key to enabling orthogonality, and this synchronization is challenging to implement in a distributed system. However, multiple access can be easily incorporated into the OFDM frame structure if the transmission is from a single transmission point to multiple receivers. At the receiver, the baseline OFDM decoding procedure is followed while only observing symbols on active carriers allocated to the data stream of interest.

B. Optical OFDM

OWC implementations commonly apply intensity modulation with direct detection (IM/DD). This restricts the transmitted waveform to a real-valued and strictly positive time domain signal. A number of adaptations to OFDM have been introduced in the literature to accommodate IM/DD, but we focus on DC-biased optical OFDM, or DCO-OFDM.

In order to meet the real-valued signal requirement, most optical OFDM techniques apply Hermitian Symmetry such that the symbol mapping first places data symbols and pilot carriers on the positive subcarriers and then directly applies the complex conjugate of each positive subcarrier to the corresponding negative subcarrier. With this complex conjugate symmetry in the frequency domain, the IFFT will generate a real-valued time domain signal. Relating to OFDMA, it is important to note that the gain of an optical transmitter drops off with frequency. As such, the active subcarrier selection plays an important role in the performance of an OWC link and, in DCO-OFDMA, inappropriate allocation of subcarriers across users can lead to performance inequities.

In order to achieve the strictly positive requirement, the transmitter can either apply a real value to the DC subcarrier during subcarrier mapping, or add a bias to the time domain electrical signal after analog conversion. In either case, the signal bias should be specified such that the signal falls within the linear response region of the optical hardware. Given that the OFDM waveform is a superposition of multiple weighted and shifted sinusoids, the signal's dynamic range must also be accounted for and the AC component of the signal should be scaled accordingly. Keeping in mind that the dynamic range is dependent on the number of superimposed sinusoids, the scaling is dependent on the number of active carriers. This is important to recognize when allocating more or less active carriers in the DCO-OFDMA implementation.

C. OWC Resource Allocation

Extending the OFDM concept to OFDMA is simple in its basic principle, but it also requires an algorithm for resource allocation. In multiple-access networks, a typical OFDMA resource allocation problem is based on assigning a subset of available subcarriers to simultaneously transmitting (and thus interfering) wireless terminals and adjusting the power associated with each active subcarrier in order to guarantee the minimum required quality of service. This idea has been applied to OFDM-based OWC, but this work is commonly evaluated via simulation. Hamouda [6] *et al.* propose a resource allocation scheme aimed at minimizing inter-cell interference in a multi-user VLC system using OFDMA. Their approach involves a two-step resource allocation process, which divides the cell coverage into two non-overlapping zones. Ling [7] *et al.* present a joint design of bias level, power, and subcarrier allocation. Wang [8] *et al.* develop a low-complexity RA algorithm for OFDMA-based LiFi systems, and Elamassie [9] *et al.* propose an adaptive algorithm that combines subcarrier allocation and bit loading to achieve uniform data rates for all nodes in the underwater sensor network.

D. SDR and gr-owc

In recent years, the widespread adoption of SDR has led to a paradigm shift in the field of RF communications. In SDRs, the signal processing stages of an RF signal chain are mostly implemented in software with ADCs/DACs and antennas being the only strictly hardware components. Consequently, SDRs have significantly reduced the barrier to entry to experimental RF research. In addition, SDRs have greatly benefited wireless communications research and education, and will continue to

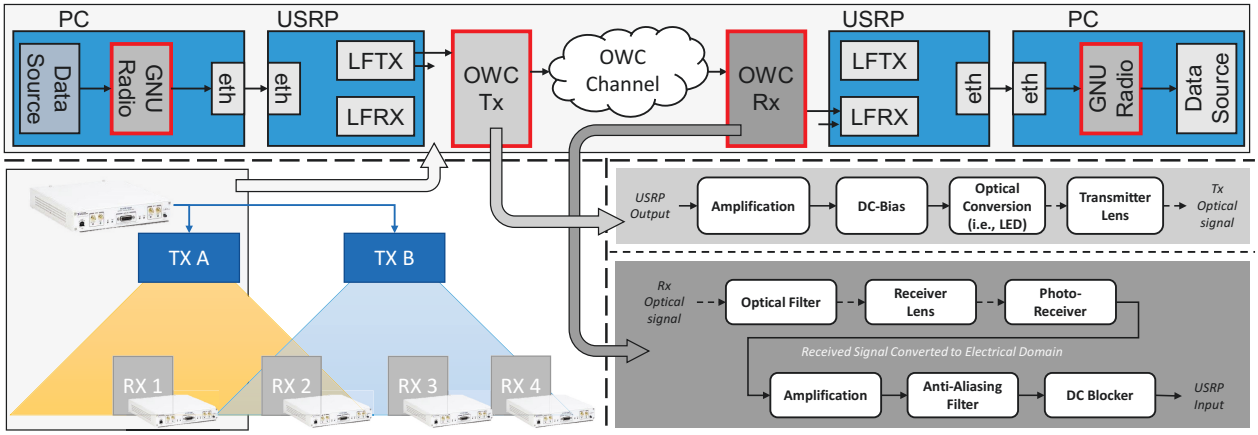

Fig. 2. Depiction of a multi-cell/multi-user SDR-Based OWC system (*bottom left*) along with a single link signal chain with modular Tx/Rx hardware (*top*) and generalized signal chains for Tx/Rx hardware (*bottom right*). In the system view, we see a need for resource allocation across users (i.e., Rx 3/4 must share the resources of Tx B) and across cells (i.e., Tx A/B must allocate resources to avoid interference at Rx 2).

do so as it is now easier and quicker than ever to move novel ideas from theory/simulation to physical implementations.

The openly available software development toolkit of GNU-Radio provides an ideal platform for SDR implementation. GNURadio provides its users the ability to build custom SDR signal processing chains, or flowgraphs, using blocks from its core library. Additionally, GNURadio supports the integration of these software flowgraphs with SDR hardware – making it incredibly simple to move between simulated and experimental environments. Furthermore, GNURadio's out-of-tree (OOT) modules allow the extension of the core functionality by enabling the inclusion of custom-made signal processing blocks.

Identifying the lack of openly available toolkits for OWC, we first published an initial version of our open source OWC signal processing toolkit in 2021. This toolkit, called *gr-owc*, is developed as an OOT module in the GNURadio framework. Our prior work on *gr-owc* describes its structure and contents in greater detail with emphasis on the developed blocks for OWC channel model and pulsed modulation schemes [2], [3]. Furthermore, readers unfamiliar with GNURadio, should go over our initial *gr-owc* paper to get a brief overview of it. Here, we will focus on our recent contributions to *gr-owc* which are related to DCO-OFDMA.

III. SDR Tools for DC-biased Optical OFDMA

GNURadio provides extensive flexibility for defining unique flowgraphs with a combination of signal processing blocks from its core library and from OOT modules, like *gr-owc*. This modularity is essential in our development of DCO-OFDM and DCO-OFDMA implementations since a subset of custom blocks (e.g., Hermitian Symmetry block) can be integrated within existing signal chains for conventional OFDM.

Beyond the extension of the single-link OFDM signal chain for DCO-OFDM, we also describe (a) the process for carrier allocation across OWC APs with overlapping coverage, and (b) the process for merging data flows at the packet level within a single OFDMA frame. The former enables dynamic resource allocation across OWC cells (e.g., TxA to Rx1 and TxB to Rx2 in Fig. 2) while the latter allows for resource allocation across multiple receivers under the coverage of a single OWC cell (e.g., TxB to Rx3 and Rx4 in Fig. 2). In order to demonstrate the setup's ability to collect extensive datasets in an automated fashion, we introduce our centrally controlled multi-node testbed architecture using XMLRPC for remote parameter control and ZMQ for remote measurements. This architecture, originally introduced in [4], allows for centralized configuration of each node's resource assignment and for parameterized data collection of packet-level performance results in various configuration settings.

A. Point to Point DCO-OFDM in gr-owc

The baseline implementation of a DCO-OFDM signal chain and simulated transmission is depicted in Fig. 3. The top image (outlined in red) shows our custom hierarchical block that takes the baseline OFDM Tx signal chain and adds our custom Hermitian Symmetry block from gr-owc. As long as the OFDM Carrier Allocator block assigns active and pilot carriers to only the positive (or only the negative) subcarriers, then our Hermitian Symmetry block takes the incoming vector of complex values and sets the negative subcarrier values equal to the complex conjugate of the corresponding positive subcarriers (or vice versa if the negative subcarriers are assigned as shown in the example flowgraph). Accordingly, the input to the IFFT block is Hermitian Symmetric and, therefore, the output time vector (as well as the output stream of the cyclic prefixer block) are real-valued - even though they are stored as complex value data types. The imaginary component of the output stream from the cyclic prefixer block is therefore dropped with the complex-to-real block, and the user-specified scaling is applied to ensure that the peak-to-peak signal range corresponds to the linear range of any OWC hardware.

The bottom image shows a test flowgraph that uses our DCO-OFDM transmitter block along with a basic OWC channel model from our gr-owc library. Note that the chan-

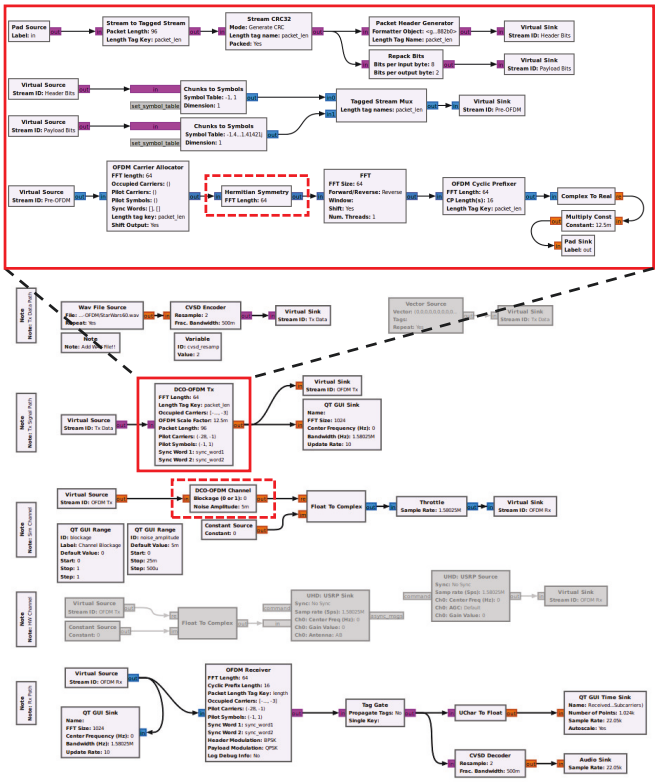

Fig. 3. Hierarchical block for DCO-OFDM (*top*) and sample flowgraph with custom modules for DCO-OFDM and a basic OWC channel (*bottom*).

nel model shown here simply allows for configurable line-of-sight (LOS) blockage and noise, but this block can be replaced with one of our other more intricate OWC channel blocks that model the specified OWC hardware along with the response relative to the position and orientation of the Tx and Rx. In this flowgraph, we have configurable options for the Tx data – namely, an audio file, fixed byte stream, or data file (not shown here). The flowgraph can also be configured for simulation or experimental testing with USRP hardware in a loopback configuration. The first important observation from the flowgraph is that we do not require a custom OFDM receiver block. Using the OFDM receiver block from GNURadio's core library, we are able to specify the relevant occupied carriers as only the positive (or only the negative) subcarriers originally defined as active carriers in the custom Tx block. The Hermitian Symmetry that was applied to generate a real-valued signal can be ignored at the receiver. The second observation here is that the output of our DCO-OFDM Tx block is a real-valued stream (as discussed above) and therefore the OWC channel block assumes a real-valued input and output stream as well. Relating to the forthcoming hardware discussion, this implies that the real-valued signal stream can be directly applied to modulate the intensity of the OWC Tx hardware, without requiring any carrier modulation by the USRP hardware.

In order to evaluate packet-level performance under various conditions, we use the file source and file sink options to transmit a file with 10000 lines where each line consists of 96 Bytes (i.e., the packet length used in our OFDM implementation). Accordingly, the received file has $10000 - N_{err}$ lines, where N_{err} is defined as the number of packets lost in transmission and the packet error rate (PER) is $N_{err}/10000$. To automate the process, we use GNURadio parameters to specify the results file name on every execution of the flowgraph. The parameterized filename allows a bash script to cycle through multiple iterations and multiple flowgraph configurations (e.g., occupied carrier selection) such that a collection of received files are saved. These files are post-processed to evaluate the distribution of PER values for each configuration across a user-specified number of iterations.

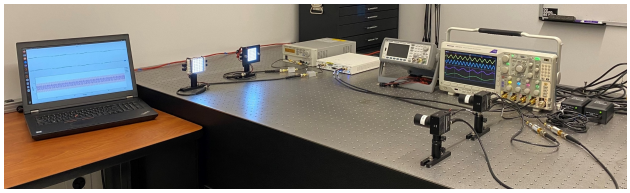

Fig. 4. Experimental setup showing a 2-Tx / 2-Rx configuration with Tx signals from USRP hardware and Rx Signals connected to Oscilloscope.

Extending this to an experimental setup, we use our testbed depicted in Fig. 4. The picture shows an instance where a single USRP X310 is used to drive 4 unique real-valued signals from a set of two LFTX daughterboards. Given the absence of a carrier modulator for OWC, we are able to directly pull from the I and Q lines of each LFTX, enabling 2 OWC transmissions from each of the X310's RF signal chains (i.e., a total of 4 OWC transmissions). In Fig. 4, we show an instance with 2 Tx signals passed through RF Bias Tees to generate the strictly positive signal that drives the LEDs. The other 2 signals are directly connected to the oscilloscope, but could also be used to drive additional LEDs. At the receiver, we have 2 Thorlab APDs with optical lenses and blue light filters. After the APD, the electrical signals are passed through a 5MHz low pass filter and DC blocking capacitor, and then connected to the oscilloscope to visually see the 4 unique tones.

When testing with over-the-air transmission and real-time Rx signal chains, the received signals are alternatively connected to another X310 USRP in a similar configuration as the transmitter configuration described above, but using LFRX daughter cards. In this case, the flowgraph from Fig. 3 is broken into two separate flowgraphs that are run independently on the Tx and Rx compute nodes. Each compute node is connected to its corresponding USRP for transmission and reception. To automate the data collection process in this configuration, the receive flowgraph is set to run continuously while a script on the transmitter's compute node cycles through multiple configurations and iterations of the flowgraph as described above. In order to generate unique receive files for each iteration/configuration, we utilize the XMLRPC library (and GNURadio's XMLRPC server functionality in the receiver's flowgraph) to remotely update the Rx filename after every completed file transmission.

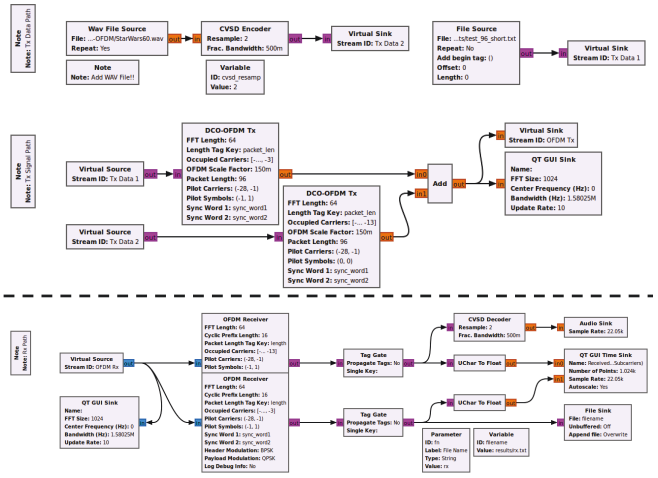

Fig. 5. DCO-OFDMA Tx and Rx flowgraphs. Separate sets of occupied carriers are used to distinguish between different data streams or users.

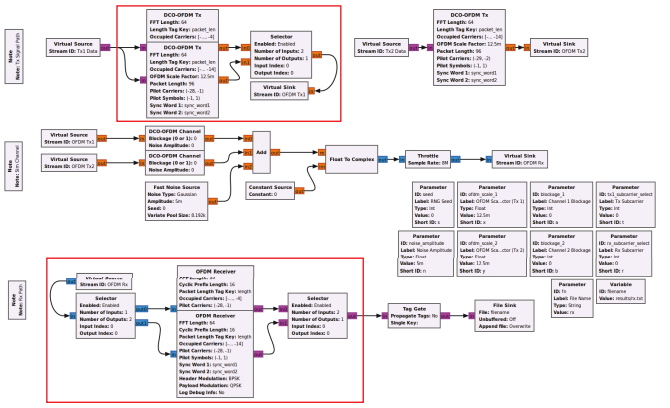

Fig. 6. DCO-OFDMA simulation flowgraph for an environment with two overlapping OWC cells. Separate sets of pilot carriers and occupied carriers are used to allocate resources across transmitters. Selector blocks allow for configuration of the subcarrier set applied at Tx 1 and observed at the Rx.

B. DCO-OFDMA Extension and Subcarrier Allocation

Using the baseline DCO-OFDM signal chain described above, we can adapt the subcarrier assignment in order to implement multi-user transmission from a single OWC AP and/or multiple simultaneous transmissions from overlapping OWC cells. In Fig. 5, we show the Tx and Rx signal chains for a **multi-user implementation** where we have two different data streams (i.e., an audio stream and a file transfer) simultaneously transmitted from a single transmitter with unique allocation of subcarriers for each stream. This is implemented with two instances of our custom DCO-OFDM Tx block, each assigned a unique set of occupied carriers, and then adding together their output signals. To avoid overemphasizing pilot carriers, only one of the OFDM Tx blocks is assigned non-zero pilot carrier symbols and the receiver for either stream will look for those symbols as their pilots. At the receiver, we simply apply multiple instances of the baseline OFDM Rx block, with each block assigned a set of occupied carriers that correspond to the carriers used by the desired Tx stream. In this visual, both streams are decoded on the same device, but a multi-user implementation can just as easily be created where each Rx device uses one of the signal chains from the flowgraph shown here.

Fig. 6 shows an instance of the DCO-OFDM module being used to simulate a **multi-cell implementation**. The main difference between this and the multi-user implementation from Fig. 5 is that the simulated waveforms are added together after separate channel blocks where each channel block represents the unique path from the corresponding transmitter to the specified receiver. Given the lack of significant multi-path in OWC, along with the relatively short distances traveled for indoor OWC, we ignore the propagation timing differences between the two paths in the simulation. In this case, the transmitter blocks are each assigned a different set of subcarriers along with unique pilot carriers. We also demonstrate the ability to configure the subcarrier set used by transmitter 1 and the observed subcarrier set at the specified receiver. This is done by using the selector blocks highlighted in the figure, and allows the selected subcarrier set to be modified as the flowgraph is running or when the flowgraph is initiated using GNURadio's parameter functionality. The parameters shown in the figure also allow the channel characteristics to be configured when the flowgraph is initiated, enabling our test automation to run through multiple scenarios/iterations in an external script. After each flowgraph execution, the received file is stored with a naming convention related to the current scenario/iteration. The set of files can be observed after all instances are complete in order to evaluate the PER performance from each scenario/iteration. As a minor note of interest, we also specify the seed value of the random noise source using a parameter. The seed value is randomly set for each iteration of a specific scenario since we found that not doing so would lead to the exact same PER in each iteration.

Finally, the simulations described above are easily converted for experimental testing by removing the channel blocks and separating the Tx/Rx signal chains into multiple flowgraphs. For the transmitters, all Tx waveforms are generated at the same compute node. When multiple users are operating in the same cell, the Tx signal chain from Fig. 5 is used. For multi-cell scenarios, we can transmit up to four unique OWC signals from a single USRP X310 using the techniques described in our prior work [4]. At the Rx node(s), each receiver applies the baseline OFDM Receiver signal chain with the OFDM Receiver block specified for the desired set of occupied carriers and the pilot carriers corresponding to the associated Tx. Automated data collection for multiple scenarios/iterations also requires some additional changes in the experimental configuration – particularly when different compute nodes are used for the Tx and Rx flowgraphs. At the Tx node, multiple scenarios/iterations can be cycled through with unique parameterized calls to initiate the Tx flowgraph (similar to what was done in the simulation). However, the Rx flowgraph can not be configured to run to completion since the Rx

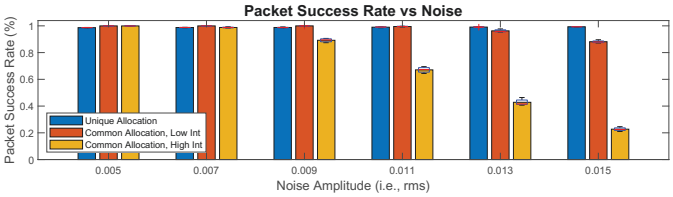

Fig. 7. Simulated packet success rate versus noise results demonstrating the impact of interference power and carrier assignment.

hardware continues to generate samples after the Tx flowgraph finishes sending the file. Accordingly, we use the XMLRPC functionality in GNURadio to create an XMLRPC server at the Rx node(s) and connect all compute nodes over a separate control network. This way, the data collection script on the Tx node can use XMLRPC to remotely configure the parameters of the Rx node(s) while the Rx flowgraphs are running. Furthermore, after each execution of the Tx flowgraph, XMLRPC can be used to update the filename used by the file sink in the flowgraphs at each Rx node.

IV. Results and Analysis

The main contribution of this work is the functionality to test multi-user and multi-cell DCO-OFDMA, but we also include some example results to demonstrate the capabilities of our tools within gr-owc. Specifically, we highlight baseline results from simulation and from the experimental setup depicted in Fig. 4. First off, Fig. 7 depicts the results of a simulated multi-cell environment using the flowgraph from Fig. 6. The specific signal, noise, and interference settings are somewhat arbitrary; but the results demonstrate the multi-cell DCO-OFDMA functionality along with some general trends of interest. Namely, at the observed noise levels the simultaneous transmission on separate carriers allows for near-perfect transmission. However, when both Txs are set to use the same subcarriers the PER begins to increase at the higher noise values. Furthermore, when the interference power is increased by increasing the simulated Tx2 gain, the PER drop off over the same noise range is more significant.

As a demonstration of the experimental setup, Table I shows a similar set of results for the deployment in Fig. 4. Here, we highlight the DCO-OFDMA functionality by comparing packet success rate of the baseline single-link DCO-OFDM implementation with the multi-cell and multi-user extensions. In the all cases, higher frequency subcarriers were assigned to the primary link that evaluated packet success rate. For the multi-cell and multi-user scenarios, we simultaneously use a set of lower frequency subcarriers to stream an audio file. The multi-cell scenario shows comparable performance to the single user instance when unique subcarriers are assigned to each cell, even though the second transmitter is within view of the primary receiver. The multi-user scenario shows a small increase in PER, but this is related to the additional scaling required due to the wider dynamic range of the OFDM waveform when additional subcarriers are active.

TABLE I
Experimental Results - Packet Success Rate

Scenario	Itertion 1	Iteration 2	Iteration 3
Single User	99.40%	99.54%	99.44%
Multi-User	97.08%	97.08%	97.15%
Multi-Cell (Unique)	99.47%	99.66%	99.57%
Multi-Cell (Common)	57.01%	56.33%	57.12%

V. Summary

As researchers continue to expand the capabilities of indoor OWC systems, experimental test capabilities are key to bridging the gap between theoretical systems and practical deployments. This work, and the baseline results presented in this paper, provide a foundational architecture for future experimentation in multi-cell / multi-user OWC systems along with reference performance metrics for comparison with novel multiple-access methodologies in the future. More details about the tools described in this paper can be found in the gr-owc public repository on GitHub. However, we note that this repository is currently under development as the codebase is being modified from compatibility with GNURadio version 3.8 to version 3.10. Documentation for the work described in this paper can be found in the final 3.8 release, but documentation and DCO-OFDM(A) examples for 3.10 will be released soon.

Acknowledgment

This work was partially supported by the National Science Foundation (NSF) ERI Program under Grant No. 2347514, the Department of Defense (DOD) under Instrumentation Grant No. W911NF2110210, and the 2022/23 Air Force Research Lab (AFRL) Beyond 5G Student Challenge.

References

[1] J. Armstrong, "OFDM for optical communications," *Journal of lightwave technology*, vol. 27, no. 3, pp. 189–204, 2009.

[2] A. Ahmed and M. B. Rahaim, "gr-owc: An open source gnuradio-based toolkit for optical wireless communications," in *2021 17th International Conference on Wireless and Mobile Computing, Networking and Communications (WiMob)*, 2021, pp. 48–53.

[3] A. Ahmed, G. Dzhezyan, H. Aboutahoun, V. Chu, J. DiViccaro, V. Ohanian, S. Rezaeiboroujerdi, I. Saheb, E. Urban, J. Wu, M. Kulhandjian, H. Kulhandjian, and M. Rahaim, "SDR beyond radio: An OOT GNU Radio library for simulation and deployment of multi-cell/multi-user optical wireless communication systems," in *GNU Radio Conf.*, 2022.

[4] C. Onwuchekwa, M. AminuMukhtar, A. Lemus, L. Martinez, V. Planchart, F. Semash, K. Kerby-Patel, H. Zhang, and M. Rahaim, "Design and implementation of a multi-node optical wireless communication testbed for centralized configuration and adaptation of system parameters using GNURadio's XML-RPC and ZMQ modules," in *GNU Radio Conf.*, 2023.

[5] F. Frederiksen and R. Prasad, "An overview of OFDM and related techniques towards development of future wireless multimedia communications," in *Proceedings RAWCON.*, 2002, pp. 19–22.

[6] M. Hammouda, A. M. Vegni, H. Haas, and J. Peissig, "Resource allocation and interference management in OFDMA-based VLC networks," *Physical Communication*, vol. 31, pp. 169–180, 2018.

[7] X. Ling, J. Wang, Z. Ding, C. Zhao, and X. Gao, "Efficient OFDMA for LiFi downlink," *Journal of Lightwave Technology*, vol. 36, no. 10, pp. 1928–1943, 2018.

[8] Y. Wang, X. Wu, and H. Haas, "Resource allocation in LiFi OFDMA systems," in *GLOBECOM*. IEEE, 2017, pp. 1–6.

[9] M. Elamassie, M. Karbalayghareh, F. Miramirkhani, M. Uysal, M. Abdallah, and K. Qaraqe, "Resource allocation for downlink OFDMA in underwater visible light communications," in *2019 BlackSeaCom*. IEEE, 2019, pp. 1–6.